The Journal of Veterinary Medical Science

NOTE

Pathology

Cervical ganglioneuroblastoma in a new born Japanese Black calf

Chun-Ho PARK[1)]*, Nozomi SHIWA[1)], Kazunori KIMITSUKI[1)], Takehito KAKIZAKI[2)] and Daisaku WATANABE[3)]

[1)]Department of Veterinary Pathology, School of Veterinary Medicine, Kitasato University, 23-35-1, Higashi, Towada, Aomori 034-8628, Japan
[2)]Department of Veterinary Radiology, School of Veterinary Medicine, Kitasato University, 23-35-1, Higashi, Towada, Aomori 034-8628, Japan
[3)]Department of Clinical Veterinary Medicine for Large Animal, School of Veterinary Medicine, Kitasato University, 23-35-1, Higashi, Towada, Aomori 034-8628, Japan

J. Vet. Med. Sci.
80(5): 755–759, 2018
doi: 10.1292/jvms.17-0694

Received: 19 December 2017
Accepted: 26 February 2018
Published online in J-STAGE: 9 March 2018

ABSTRACT. This case report describes a congenital ganglioneuroblastoma in a 38-day-old male Japanese Black calf. The cervical multinodular mass was present at birth and grew rapidly. The cut surface was pale gray-to-yellow and had a gelatinous appearance. Hemorrhagic cysts of various sizes were observed in the nodule. Histologically, the mass contained clusters of neuroblastic cells, ganglionic cells, and Schwann-like cells. Immunohistochemically, the ganglionic cells showed strong positivity for neuron-specific enolase, neurofilament, synaptophysin, and chromogranin A, whereas the Schwann-like cells strongly expressed S-100, glial fibrillary acidic protein, and vimentin. Ultrastructurally, neurosecretory granules resembling catecholamine were observed in the neuroblastic and Schwann-like cells. Based on the pathology, the diagnosis was congenital cervical nodular ganglioneuroblastoma.

KEY WORDS: calf, case report, cervical nodular ganglioneuroblastoma, congenital, diagnosis

Peripheral neuroblastic tumors are classified as neuroblastomas, ganglioneuroblastomas, and ganglioneuromas [1]. Neuroblastoma resembles the fetal adrenal medulla and is characterized by uniform small round cells with central chromatin-rich nuclei and faintly staining cytoplasm. Rosette patterns may be visible in some cases. Ganglioneuroblastoma has primitive neuroblasts along with maturing ganglion cells; the number and arrangement of the cells vary, so the tumor assumes a wide range of appearances and is associated with a broad spectrum of biologic behavior. Ganglioneuroma has the features of mature differentiated nerve cells, i.e., vesicular nuclei with a prominent nucleolus, cytoplasmic Nissl bodies, and a Schwannian matrix [13]. These tumors are of neuronal lineage and are believed to originate from neural crest cells in the sympathetic nervous system and arise wherever sympathetic nervous system tissue exists. In humans, most peripheral neuroblastic tumors occur in the cranial and spinal nerve ganglia, adrenal gland, posterior mediastinum, retroperitoneum, and pelvis [8]. Neuroblastoma [11], ganglioneuroblastoma [18], and ganglioneuroma [15] have been reported in cattle; however, to our knowledge, there has been no report of congenital ganglioneuroblastoma.

The subject of this case report was a calf (Japanese Black, male, aged 38 days) that was presented with a cutaneous cervical mass. The mass had been present at birth (Fig. 1). Despite progressive enlargement of the mass, the calf had a good appetite and appeared healthy. However, the mass continued to grow steadily until it was pressing on the upper airway and esophagus. The calf was euthanized at 38 days of life because of a poor prognosis and submitted for necropsy. The mass (approximately, 25 × 20 cm) was found to be located mainly in the right cervical subcutis and was composed of multiple nodules that varied in size. The largest nodule was 15 × 8 cm and surrounded by thick connective tissue. The cut surface was pale gray-to-yellow and had a gelatinous appearance. Hemorrhagic cysts of various sizes were observed (Fig. 2). Hemorrhagic foci tended to form in the center of the nodule. Small nodules had infiltrated the lower jaw, pharynx, and soft palate, but infiltration into the cervical spine and facial bones was not observed. Mild bronchopneumonitis was present in the lungs, but no other gross findings of note were detected in the other major organs (brain, liver, spleen, heart, kidneys).

The mass was embedded in paraffin wax and cut into 3-μm thick sections. The sections were stained with hematoxylin and eosin. Immunohistochemical analyses were performed using the polymer method with EnVision+ (Dako, Glostrup, Denmark). The primary antibodies used in these experiments were as follows: glial fibrillary acidic protein (GFAP, Nichirei Biosciences Inc., Tokyo, Japan; prediluted), neurofilament protein (NF, Dako; prediluted), myelin basic protein (Nichirei; prediluted),

*Correspondence to: Park, C.-H.: baku@vmas.kitasato-u.ac.jp

neuron-specific enolase (NSE, Dako; prediluted), S-100 protein (Nichirei; prediluted), synaptophysin (Nichirei; prediluted), nestin (BioLegend; 1:200), tyrosin hydroxylase (TH) (GeneTex; 1:2,500), chromogranin A (Nichirei; prediluted), vimentin (Nichirei; prediluted), and cytokeratin (AE1/AE3, Dako; prediluted). To investigate the proliferation rate of the tumor cell population, nucleoli positive for Ki-67 MIB-1 (Dako; prediluted) were scored by counting at least 1,000 cells in representative 400 × high-power fields. The antigen-antibody complexes were visualized using 3-3′-diaminobenzidine solution (Dako), and the sections were counterstained with hematoxylin. The formalin-fixed specimen was cut into 1-mm blocks, fixed in 1% buffered osmium tetroxide, and embedded in epoxy resin. Sections approximately 70 nm in thickness were stained with uranyl acetate and lead citrate, and examined using a transmission electron microscope (H-7650, Hitachi, Tokyo, Japan).

Microscopically, the mass was composed of small and large nodules. Each nodule contained densely and poorly cellular areas separated by fibrovascular stroma (Fig. 3), and showed a trabecular or whorled growth pattern. Densely cellular areas were present in the center of the nodule and composed of irregular sheets of poorly differentiated neuroblastic cells and poor stroma (Fig. 4). These cells contained a moderate amount of eosinophilic cytoplasm and nuclei with a round-to-polygonal shape and one or two prominent nucleoli. Anisocytosis and anisokaryosis were marked, and occasionally mitotic figures were observed. The hypocellular areas were composed of ganglionic cells, Schwann-like cells, and abundant connective stroma. The ganglionic cells contained large round nuclei with a single nucleolus, abundant eosinophilic cytoplasm, and coarsely granular basophilic cytoplasmic components that resembled Nissl substance (Fig. 5). Individual or small nests of ganglion cells were separated by Schwann-like cells, which contained small round-to-elliptical nuclei with indistinct nucleoli. The majority of the Schwann-like cells had perinuclear halos resembling oligodendroglia in a fibrillary Schwann-like stroma (Fig. 6). Mitotic figures were not observed in either the ganglionic or Schwann-like tumor cells.

Immunohistochemically, the neuroblastic cells were positive for NSE, synaptophysin, nestin, TH, S-100, and chromogranin A, but were negative for NF, GFAP, vimentin, myelin basic protein, and cytokeratin AE1/AE3. The ganglionic cells were positive for NSE, NF, synaptophysin, nestin (Fig. 7), TH, and chromogranin A, but were negative for other antibodies. The Schwann-like cells were strongly positive for S-100 (Fig. 8), GFAP, nestin, TH, and vimentin, but expression of NSE, NF, and synaptophysin was weakly detected. Strong nuclear Ki-67 immunoreactivity was detected in the neuroblastic cells, especially near the hemorrhagic areas in the center of the nodule. The Ki-67 proliferation index was 65% in the neuroblastic cells but was less than 5% in the ganglionic and Schwann-like cells. The immunoreactivity results for the tumor cells are summarized in Table 1.

Ultrastructurally, the neuroblastic cells had elongated cytoplasmic processes that were sometimes intertwined (Fig. 9). These cytoplasmic processes varied in size (from 50 nm to 2 μm in length and from 100 to 300 nm in width). Neurosecretory granules (50–100 nm in diameter) with membrane-bound dense-core granules, flask-shaped caveola-like invagination of the cell membrane (Fig. 9, insert A), microtubes (Fig. 9, insert B), and neurofilaments (Fig. 9, insert C), were observed, along with a small number of cell organelles. The ganglionic cells were embedded in a matrix and contained abundant rough endoplasmic reticulum, free ribosomes, Golgi apparatus and a few neurosecretory granules. The Schwann-like cells were separated by variable amounts of collagen fibers and basal membrane and had long cytoplasmic processes. The nucleus was small and round to ellipsoid in shape, and no nucleoli could be observed. Neurosecretory granules and unmyelinated axons containing mitochondria were frequently observed (Fig. 10).

The tumor in our calf consisted of three components, i.e., neuroblastic cells, ganglionic cells, and Schwann-like cells, and showed multinodular growth patterns. The largest population was of Schwann-like cells, followed by neuroblastic cells and ganglionic cells. Sometimes, these cell types were intermixed in the same nodule. The tumor was very large in our case and proliferated invasively into the neck, to the extent that the origin of the tumor could not be identified. Peripheral neuroblastic tumors originate from sympathetic progenitor cells, which in turn are derived from neuroectodermal stem cells [10]. Nestin is an intermediate filament protein that is expressed in neuroectodermal stem cells in early development [7]. Nestin is also detected in some brain tumors such as neuroblastoma and other primitive neuroectodermal tumors [14]. In our case, nestin was positive in neuroblastic and Schwann-like cell components, but ganglion cells were negative. Therefore, it was suggested that neuroblastic and Schwann-like cells may originated from primitive neuroectodermal stem cells and were immature cells. Vagal neuroectodermal stem cells give rise to most of the parasympathetic and superior sympathetic cervical ganglia. TH is the rate limiting enzyme in catecholamine synthesis and is found in catecholamine producing cells such as sympathetic ganglia [16] and sensory ganglia [6]. In our case, TH was positive in ganglionic cells, so, it was suspected that the likely origin of the tumor in this case was vagal neuroectodermal stem cells.

The immunoreactivity patterns excluding nestin and TH seen in this calf are similar to those previously reported for bovine intestinal ganglioneuroblastoma [18]. However, the results of immunoreactivity tests for NSE, synaptophysin and GFAP in the neuroblastic and Schwann cell-like cells in that report are not consistent with those in our case. In the previous report, neuroblastic and Schwann-like cells was immunonegative for NSE and synaptophysin, and only a few Schwann-like cells were immunopositive for GFAP. Besides, in the present case neuroblastic cells showed moderate immunoreactivity for NSE and synaptophysin, and the Schwann-like cells showed diffuse and intense immunoreactivity for GFAP. Therefore, it was speculated that the different patterns of immunoreactivity might be related to differences in the degree of differentiation of tumor cells. Ki-67 is a marker of cell proliferation and is used widely to predict tumor behavior and surgical outcomes [3]. In the present case, Ki-67 expression was mainly observed in the neuroblastic component in the center of the nodule, suggesting that neuroblastic cells were the most primitive tumor cells and that the ganglionic and Schwann-like cells may have differentiated from the neuroblastic cells. It has been reported that neuroblasts can mature into more highly differentiated forms, such as neurons and Schwann cells [2, 17]. Our findings in this case support that hypothesis.

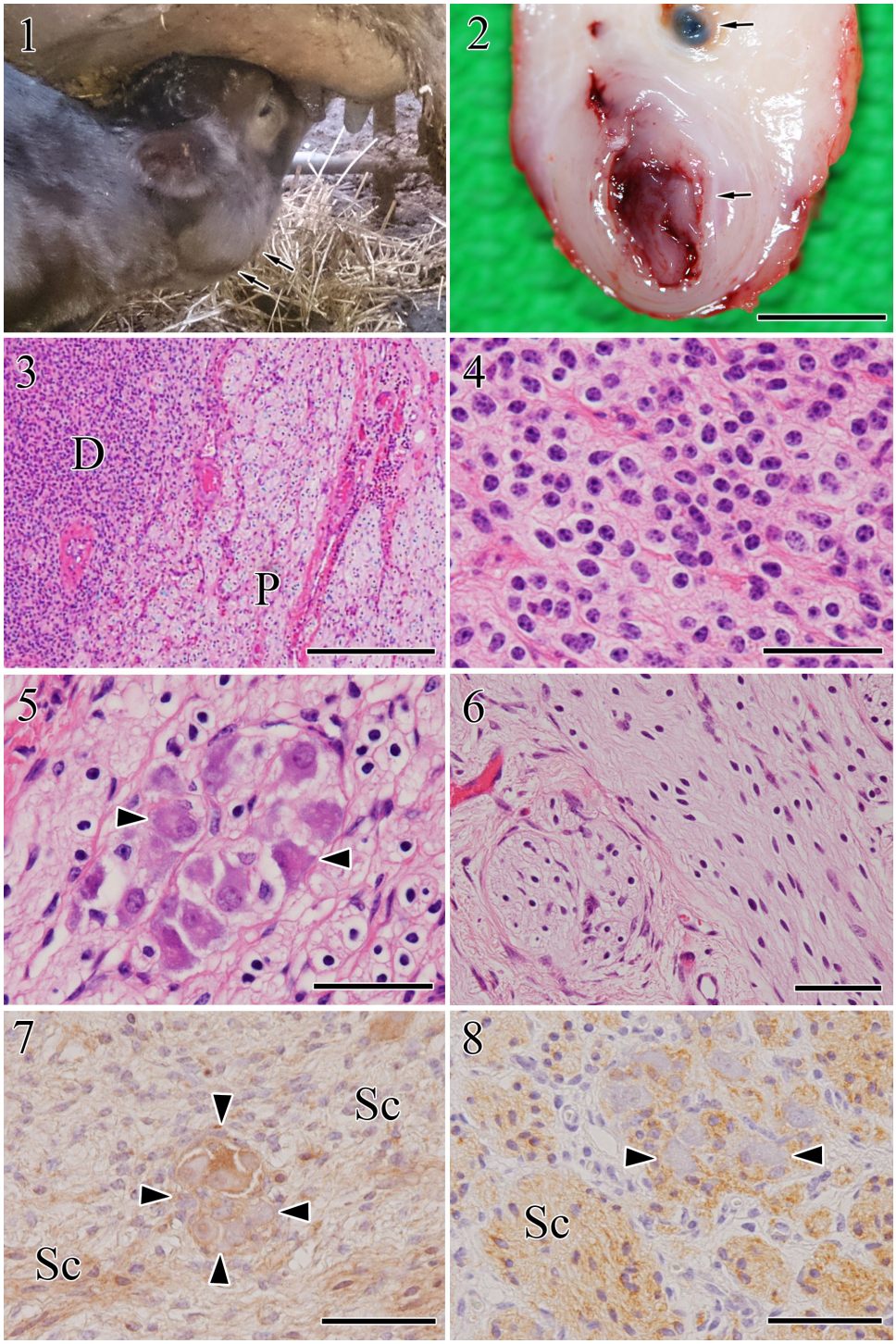

Fig. 1. Gross findings for a large nodular cervical mass (arrows) extending from the mandible to the cervical neck at birth.

Fig. 2. Cut surface findings for the cervical mass. The cut surface is pale gray-to-yellow, gelatinous, and contains hemorrhagic cysts (arrows) of various sizes. Bar=1 cm.

Fig. 3. Microscopically, the cervical mass composed of densely (D) and poorly (P) cellular areas separated by fibrovascular stroma. Hematoxylin and eosin staining. Bar=250 μm.

Fig. 4. Densely cellular areas within the cervical mass are composed of sheets of undifferentiated neuroblastic cells. Hematoxylin and eosin staining. Bar=25 μm.

Fig. 5. The hypocellular areas of the cervical mass are composed of separated ganglionic cells (arrowheads), Schwann-like cells, and connective stroma. Hematoxylin and eosin staining. Bar=25 μm.

Fig. 6. The hypocellular areas of the cervical mass are mainly composed of Schwann-like cells. Hematoxylin and eosin staining. Bar=50 μm.

Fig. 7. Ganglionic cells (arrowheads) and Schwann-like cells (Sc) are positive for nestin. Immunohistochemistry. Bar=50 μm.

Fig. 8. Schwann-like cells (Sc) are positive for S-100, but ganglionic cells (arrowheads) are negative. Immunohistochemistry. Bar=50 μm.

Table 1. Primary antibodies used for the immunohistochemical examination and results

Antibody	Source	Host	Dilution	Antigen retrieval	Ganglionic	Neuroblastic	Schwannian
Chromogranin A	Nichirei	Rabbit	Prediluted	MW, 170 W, 10 min	+++	++	-
NF	Dako	Mouse	Prediluted	Pro-K, 37°C, 10 min	+++	-	+
NSE	Dako	Mouse	Prediluted	MW, 170 W, 10 min	+++	++	+
Synaptophysin	Nichirei	Mouse	Prediluted	AC, 121°C, 10 min	+++	++	+
Nestin	BioLegend	Rabbit	1:200	No treatment	+	++	++
TH	GeneTex	Rabbit	1:2,500	No treatment	+	++	++
GFAP	Nichirei	Rabbit	Prediluted	No treatment	-	-	+++
S-100	Nichirei	Rabbit	Prediluted	No treatment	-	++	+++
Vimentin	Nichirei	Mouse	Prediluted	MW, 170 W, 10 min	-	-	+++
Cytokeratin	Dako	Mouse	Prediluted	Pro-K, 37°C, 5 min	-	-	-
MBP	Chemicon	Rabbit	1:200	Pro-K, 37°C, 10 min	-	-	-
Ki-67	Dako	Mouse	Prediluted	AC, 121°C, 10 min	0%	65%	5%

+++, diffuse and strong; ++, moderate; +, focal and strong; -, negative. AC, autoclave; GFAP, glial fibrillary acidic protein; MBP, myelin basic protein; MW, microwave; NF, neurofilament protein; NSE, neuron-specific enolase; Pro-K, proteinase K; TH, tyrosine hydroxylase.

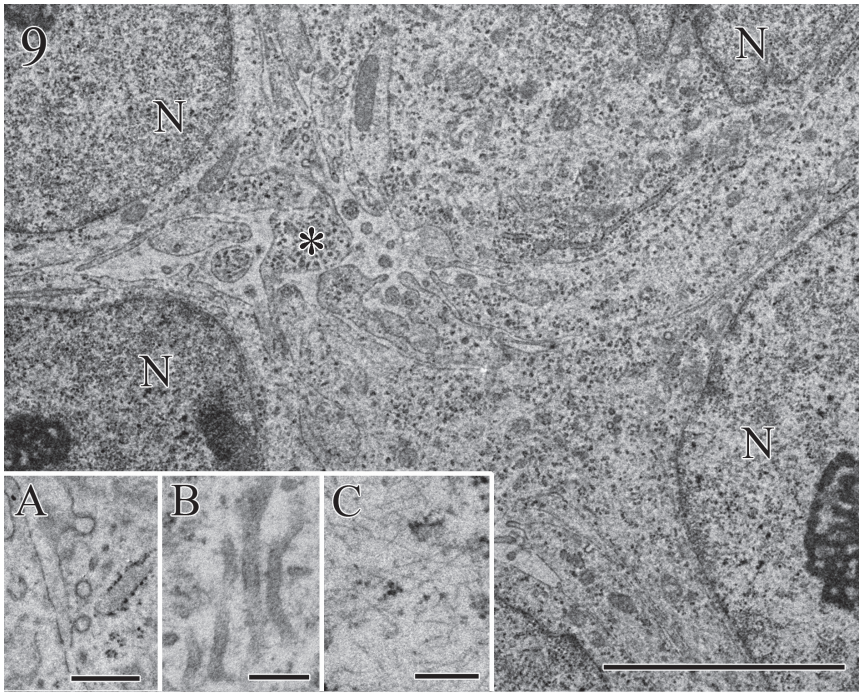

Fig. 9. Ultrastructurally, the cervical mass contains neuroblastic cells with elongated cytoplasmic processes that are intertwined with each other (*). Flask-shaped caveola-like invaginations (insert A), microtubes (insert B), and neurofilaments (insert C) are observed in the cytoplasm. N, nucleus. Transmission electron microscopy. Bar=1 μm (A, 500 nm; B, C=200 nm).

Generally, ultrastructural findings for neuroblastic tumors include dense-core granules in the cytoplasm, neural processes containing neurofilaments, neurotubules, mitochondria, and neurosecretory granules [9]. In our case, neurosecretory granules were observed more frequently in the neuroblastic and Schwann-like cells [4] than in the ganglionic cells; however, organelles such as the rough endoplasm reticulum and Golgi apparatus were the most developed in the ganglionic cells. Therefore, we consider that ganglionic cells were the more maturated component in this tumor.

According to the classification system used for human tumors, ganglioneuroblastoma is subdivided into two categories, i.e., nodular and intermixed, on the basis of the type of neuroblastoma component [5, 12]. Shimada *et al.* [13] have proposed that the term “nodular ganglioneuroblastoma” should be restricted for tumors that contain a Schwannian component, ganglion cells, and a neuroblastic component. In addition, at least one well circumscribed nodule of neuroblasts and hemorrhagic nodules should be included in the gross specimen. According to these criteria, the findings in our present case were consistent with nodular ganglioneuroblastoma. To our knowledge, this is the first report of congenital ganglioneuroblastoma in a calf.

ACKNOWLEDGMENTS. This case was presented at the 56th veterinary pathology slide forum in Japan.

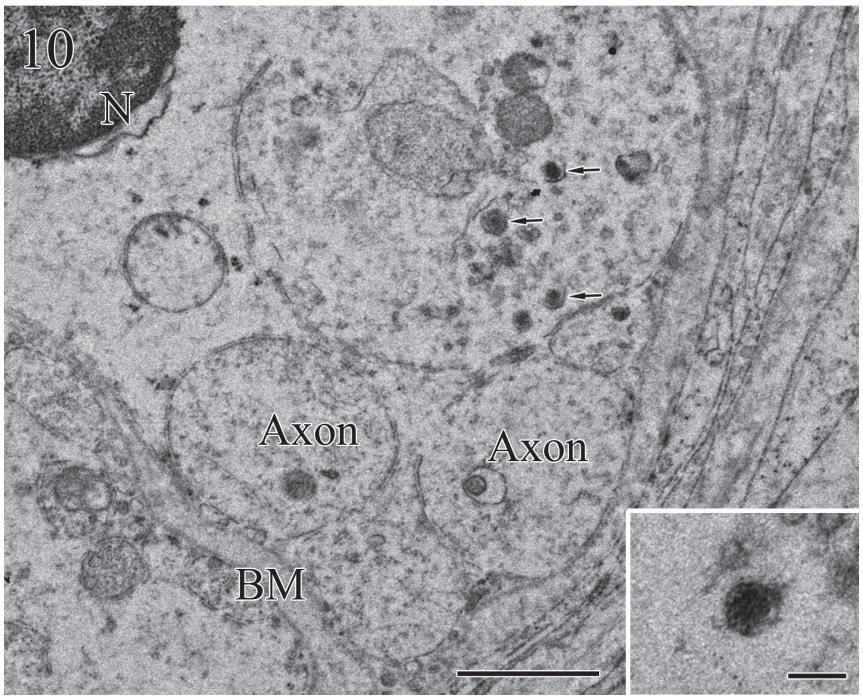

Fig. 10. Neurosecretory granules (arrows and insert), unmyelinated axons, and BM are observed in the Schwann-like cells in the cervical mass. BM, basal membrane; N, nucleus. Transmission electron microscopy. Bar=1 μm.

REFERENCES

1. Cantile, C. and Youssef, S. 2016. Nervous system. pp. 405–406. *In*: Pathology of Domestic Animals, 6th ed., vol. 1 (Maxie, M. G. ed.), St. Louis.
2. de Chadarévian, J. P., Montes, J. L., O'Gorman, A. M. and Freeman, C. R. 1987. Maturation of cerebellar neuroblastoma into ganglioneuroma with melanosis. A histologic, immunocytochemical, and ultrastructural study. *Cancer* **59**: 69–76. [Medline] [CrossRef]
3. Gerdes, J., Lemke, H., Baisch, H., Wacker, H. H., Schwab, U. and Stein, H. 1984. Cell cycle analysis of a cell proliferation-associated human nuclear antigen defined by the monoclonal antibody Ki-67. *J. Immunol.* **133**: 1710–1715. [Medline]
4. Hicks, M. J. and Mackay, B. 1995. Comparison of ultrastructural features among neuroblastic tumors: maturation from neuroblastoma to ganglioneuroma. *Ultrastruct. Pathol.* **19**: 311–322. [Medline] [CrossRef]
5. Joshi, V. V., Cantor, A. B., Altshuler, G., Larkin, E. W., Neill, J. S., Shuster, J. J., Holbrook, C. T., Hayes, F. A. and Castleberry, R. P. 1992. Recommendations for modification of terminology of neuroblastic tumors and prognostic significance of Shimada classification. A clinicopathologic study of 213 cases from the Pediatric Oncology Group. *Cancer* **69**: 2183–2196. [Medline] [CrossRef]
6. Katz, D. M. and Erb, M. J. 1990. Developmental regulation of tyrosine hydroxylase expression in primary sensory neurons of the rat. *Dev. Biol.* **137**: 233–242. [Medline] [CrossRef]
7. Lendahl, U., Zimmerman, L. B. and McKay, R. D. 1990. CNS stem cells express a new class of intermediate filament protein. *Cell* **60**: 585–595. [Medline] [CrossRef]
8. Lonergan, G. J., Schwab, C. M., Suarez, E. S. and Carlson, C. L. 2002. Neuroblastoma, ganglioneuroblastoma, and ganglioneuroma: radiologic-pathologic correlation. *Radiographics* **22**: 911–934. [Medline] [CrossRef]
9. Misugi, K., Misugi, N. and Newton, W. A. Jr. 1968. Fine structural study of neuroblastoma, ganglioneuroblastoma, and pheochromocytoma. *Arch. Pathol.* **86**: 160–170. [Medline]
10. Mora, J. and Gerald, W. L. 2004. Origin of neuroblastic tumors: clues for future therapeutics. *Expert Rev. Mol. Diagn.* **4**: 293–302. [Medline] [CrossRef]
11. Omi, K., Kitano, Y., Agawa, H. and Kadota, K. 1994. An immunohistochemical study of peripheral neuroblastoma, ganglioneuroblastoma, anaplastic ganglioglioma, schwannoma and neurofibroma in cattle. *J. Comp. Pathol.* **111**: 1–14. [Medline] [CrossRef]
12. Peuchmaur, M., d'Amore, E. S., Joshi, V. V., Hata, J., Roald, B., Dehner, L. P., Gerbing, R. B., Stram, D. O., Lukens, J. N., Matthay, K. K. and Shimada, H. 2003. Revision of the International Neuroblastoma Pathology Classification: confirmation of favorable and unfavorable prognostic subsets in ganglioneuroblastoma, nodular. *Cancer* **98**: 2274–2281. [Medline] [CrossRef]
13. Shimada, H., Ambros, I. M., Dehner, L. P., Hata, J., Joshi, V. V. and Roald, B. 1999. Terminology and morphologic criteria of neuroblastic tumors: recommendations by the International Neuroblastoma Pathology Committee. *Cancer* **86**: 349–363. [Medline] [CrossRef]
14. Smits, A., van Grieken, D., Hartman, M., Lendahl, U., Funa, K. and Nistér, M. 1996. Coexpression of platelet-derived growth factor alpha and beta receptors on medulloblastomas and other primitive neuroectodermal tumors is consistent with an immature stem cell and neuronal derivation. *Lab. Invest.* **74**: 188–198. [Medline]
15. Sokale, E. O. and Ladds, P. W. 1983. Multicentric ganglioneuroma in a steer. *Vet. Pathol.* **20**: 767–770. [Medline] [CrossRef]
16. Teitelman, G., Baker, H., Joh, T. H. and Reis, D. J. 1979. Appearance of catecholamine-synthesizing enzymes during development of rat sympathetic nervous system: possible role of tissue environment. *Proc. Natl. Acad. Sci. U.S.A.* **76**: 509–513. [Medline] [CrossRef]
17. Tsokos, M., Scarpa, S., Ross, R. A. and Triche, T. J. 1987. Differentiation of human neuroblastoma recapitulates neural crest development. Study of morphology, neurotransmitter enzymes, and extracellular matrix proteins. *Am. J. Pathol.* **128**: 484–496. [Medline]
18. Ulrich, R., Stan, A. C., Koch, A. and Beineke, A. 2008. Expression of brain-derived neurotrophic factor and tropomyosin-related kinase-B in a bovine jejunal nodular ganglioneuroblastoma. *Vet. Pathol.* **45**: 355–360. [Medline] [CrossRef]